KADIR HAS UNIVERSITY
GRADUATE SCHOOL OF SCIENCE AND ENGINEERING

PRIMARY USER DETECTION IN ULTRAWIDE-BAND BASED WIRELESS SENSOR NETWORKS

YAĞMUR SABUCU

May, 2013

PRIMARY USER DETECTION IN ULTRAWIDE-BAND BASED WIRELESS SENSOR NETWORKS

Yağmur Sabucu

Submitted to the Graduate School of Science and Engineering
in partial fulfillment of the requirements for the degree of
Master of Science
In
Electronics Engineering

KADIR HAS UNIVERSITY
May, 2013

PRIMARY USER DETECTION IN UWB-BASED WIRELESS SENSOR NETWORKS

APPROVED BY:

Asst. Prof. Dr. Serhat Erküçük (Thesis Supervisor)	.....
Prof. Dr. Erdal Panayırcı	.....
Prof. Dr. Hakan Çırpan	.....

DATE OF APPROVAL: Day.Month.Year

PRIMARY USER DETECTION IN UWB-BASED WIRELESS SENSOR NETWORKS

ABSTRACT

With the increasing need for higher data rates and new technologies, frequency band allocation has been an essential issue. Accordingly, unlicensed usage of available spectrum has been an important research topic in the context of cognitive radios. The first step in using the available spectrum in an unlicensed way is to detect the presence/absense of the primary user. While an individual secondary user may sense the spectrum and decide on the availability of the spectrum, the detection performance will be much better if many secondary users sense the spectrum and transmit their decision to a fusion center.

In this thesis, ultra-wideband (UWB) based wireless sensor networks (WSNs) are considered for the detection of a primary user. Different from earlier works, (i) both uplink and downlink information of the primary user are assessed for the primary user detection, and (ii) IEEE 802.15.4a standard is considered for the implementation of each secondary user. Specifically, the worked focused on the comparison of the two IEEE 802.15.4a based signalling, namely, binary pulse position modulation (BPPM) and combined BPPM/ binary phase shift keying (BPPM/BPSK), and the implementation of noncoherent receivers at the fusion center for reduced complexity. Accordingly, the sensor-fusion center link is investigated in detail considering practical implementation conditions. Some suggestions have been provided based on the primary user detection performance results of the UWB based WSNs.

ULTRA GENİŞBAND TABANLI KABLOSUZ SENSÖR AĞLARINDA BİRİNCİL KULLANICI ALGILANMASI

ÖZET

Teknolojinin gelişmesiyle beraber kısıtlı frekans bandları varolan teknolojiler ile kullanıcı talebini karşılayamaz hale geldi. Buna bağlı olarak, lisanslı kullanıcının frekans bandı uygun olduğunda, lisanssız kullanıcıya erişim imkanı verilmesi önemli bir araştırma konusu haline geldi. Lisanslı bandın kullanılabilmesi için ilk adım birincil kullanıcının frekans bandının doluluk/boşluk durumunu tespit etmektir. Böyle bir sistemde, tek bir sensörün lisanslı kullanıcıyı dinlemesi yerine bir çok ikincil kullanıcının bandı dinlemeleri ve kararlarını bir füzyon merkezine yollamaları performansı çok daha fazla arttıracaktır. Bu çalışmada, ultra geniş bandlı (UGB) kablosuz sensör ağlarında birincil kullanıcı algılaması incelenmiştir. Önceki çalışmalardan farklı olarak, (i) birincil kullanıcının yer-uydu ve uydu-yer bilgilerinin her biri, birincil kullanıcı algılaması için değerlendirilmiş, (ii) her bir ikincil kullanıcının gerçeklenmesi için IEEE 802.15.4a standartı kullanılmıştır. Bu çalışmada, özellikle IEEE 802.15.4a tabanlı ikili darbe konum kiplemesi (BPPM) ve birleşik bir kipleme olan ikili faz kaymalı darbe konum kiplemesi (BPPM/BPSK) ile karmaşıklığı azaltabilmek için füzyon merkezinde evreuyumsuz alıcılara yoğunlaşılmıştır. Buna bağlı olarak, sensör-füzyon merkezi arasındaki kanalın gerçeklenmesi ayrıntılı olarak araştırılmıştır, UGB tabanlı kablosuz sensör ağlarının birincil kullanıcı algılama performans sonuçlarıyla desteklenen öneriler yapılmıştır.

ACKNOWLEDGEMENTS

Firstly of all, I want to thank my thesis supervisor, Asst. Prof. Dr. Serhat Erküçük for his support during my research and graduate studies. He always guided me with his priceless suggestions and work discipline during my master education. Additionally, I want to thank the other professors in my program and my graduate assistant friends. They always supported me with their friendship and encouraged me go through the thesis and graduate studies.

In addition, I would like to acknowledge the Department of Electronics Engineering of Kadir Has University, and Asst. Prof. Dr. Serhat Erküçük's research grant from the 7^{th} European Community Framework Programme - Marie Curie International Reintegration Grant for the financial support throughout my graduate studies. During my graduate studies, I have been a research assistant in Prof. Erküçük's project in the last two years. I also would like to thank TÜBİTAK-BİDEB for providing me financial support during my graduate studies.

Finally, I deeply thank my family especially my parents, for their patience and encouragement. I could never finish this thesis without their sacrifices.

TABLE OF CONTENTS

LIST OF FIGURES

LIST OF TABLES

LIST OF SYMBOLS/ABBREVIATIONS

CR	: Cognitive radio
WSN	: Wireless sensor network
SNR	: Signal-to-noise ratio
UWB-IR	: Ultra wideband - Impulse radio
BPPM	: Binary pulse position modulation
BPPM/BPSK	: BPPM/Binary phase shift keying
WiFi	: Wireless fidelity
WLAN	: Wireless local area network
DSSS	: Direct sequence spread spectrum
PHY	: Physical layer
MAC	: Media access control layer
FC	: Fusion center
NP	: Neyman-Pearson
TH-IR	: Time hopping-Impulse radio
DD-BPPM	: Double duration-BPPM
CM	: Channel model
AWGN	: Additive white Gaussian noise
M	: Number of bands
h_i	: ith multipath coefficient
τ_i	: delay of the ith multipath component
T_i	: Integration duration
L	: Number of multipath delay components
T_s	: Signal duration
$\delta(.)$	: Dirac delta function
L_r	: Number of rake fingers

K	: Number of sensors
$P_{e,j}$	: Probability of error for the jth case
$P_{e,m}$	: Probability of error for the mth link
$P_{f,T}$	: Total probability of false alarm for one sensor
$P_{md,T}$	: Total probability of misdetection for one sensor
$\hat{P}_f$	: The probability of false alarm for the overall system
$\hat{P}_{md}$	: The probability of misdetection for the overall system
E_p	: Pulse energy
E_b	: Energy per bit
N_f	: Number of frames
W_{rx}	: Noise bandwidth of the receiver front end
H_0	: Hypothesis that the primary system is absent
H_1	: Hypothesis that the primary system is present
λ_i	: Threshold values
χ^2	: Chi-square distribution
γ_m	: SNR of the mth channel
η	: Noise term

1. INTRODUCTION

Wireless sensor networks (WSNs) have become one of the most important technologies in recent years. WSNs have many positive aspects such as robustness, high flexibility, and low complexity. In the same manner, they can be used in many applications such as large surveillance coverage, and some security and monitoring applications for traffic, environment or battlefield.

WSNs contain many cost-efficient and power-efficient sensors that collect and process the observations for a specific environment. Each sensor in a WSN has a battery to provide itself the required energy to communicate, therefore, it has a very limited energy budget. Accordingly, energy efficient and long-life systems are very essential for WSNs. To perform this, WSNs have to be able to work under low SNR. Therefore, the studies in low SNR region are very essential for WSNs, whereas unreliable communication channels can cause a significant decrease in the system performance [1]. Sensor nodes in WSNs are capable of communicating with each other through various wireless channels that can change the overall performance essentially. Besides this, sensors typically transmit their observations to a fusion center that gathers data and makes a final decision according to these observations.

1.1. Literature on Wireless Sensor Networks

Fusion center and the decision mechanisms which are applied in it, are among the important design issues for WSNs [2]. According to one of these studies, [3] , an opportunist power allocation strategy is presented for Nakagami-m fading channel in parallel fusion WSNs. Considering the decision mechanisms, Liu and Sayeed, present a type-based multi access method which requires the number of sets for all possible observations in orthogonal multi access channels [4]. Besides allocation strategies and robustness under low SNR, many other aspects such as distributed data compression and transmission, and collaborative sig-

nal processing have been studied [5]-[7]. Some studies have investigated the optimum fusion rules which have been obtained under some assumptions such as conditional independence [8]-[9]. The distributed target detection is particularly presented in [10], and the correlated observations on decision fusion were studied in [11]-[14]. WSNs have also been defined for various applications such as consumer product, healthcare, environment, and industrial applications which are identified in [15]-[20].

Many WSNs are based on narowband transmission schemes such as frequency hopping and direct sequence with multiple access techniques [21]. On the other hand, robust communications and high-precision ranging capability properties of a WSN can be better with ultra-wideband transmission schemes.

1.2. Literature on Ultra-Wideband Based WSNs

Until recent years, classical communication approaches have been implemented for wireless communication systems. Operating simultaneously and not generating interference to each other are very crucial properties under the condition that each wireless system has its own frequency band and data transmission technique. However, considering the high demand for new wireless communication technologies, the limited licensed systems being assigned to various frequency bands, does not satisfy the high demand. As a solution, cognitive radios [22] and ultra wideband (UWB) systems [23] have been proposed as unlicensed technologies.

These unlicensed technologies have been commonly accepted for efficient utilization of the spectrum. UWB communication techniques are very useful for WSNs, due to the numerous positive aspects which are very suitable to the inherent of WSN applications. Compared to narrowband transmissions and direct sequence spread spectrum (DSSS) and WiFi technologies, UWB has various essential advantages such as low energy, low complexity and low cost structure. UWB systems also have high robustness against multi-path, and have very high time-domain resolution for some specific applications. In UWB, the signal is spread

over a very large bandwidth (generally equal to or greater than 500 MHz). Increasing the spreading factor enhances the robustness. The impulse radio uses very short duration pulses and these low duty cycle pulses result in low energy consumption. In addition, the fact that the precision of ranging requirements are proportional to the bandwidth makes UWB attractive for geo-location applications.

UWB technologies use the licensed frequency bands by transmitting data at a very low power spectral density. The main aim is to cause minimum interference to licensed systems in these frequency bands during transmission. Accordingly, if secondary users such as cognitive radios and UWB systems are sharing the same frequency band with a primary system, they have to assess the activity of a primary user before they can communicate. While a secondary user can decide individually on the presence or absence of a primary user, a decision made considering the assessment of distributed users is more reliable. Hence, primary (i.e., licensed) user detection performance of UWB systems is a widely investigated topic by wireless communications community. In WSNs, non-coherent receivers and multi access channels with distributed sensing scenario are commonly considered to decrease the usage of power under Rician and Rayleigh fading channels [24]. In [26], distributed detection in UWB based WSNs was studied considering the effect of energy requirement, bandwidth and data rate in frequency selective channels.

Of the numerous positive aspects of the systems which are based on the UWB based IEEE 802.15.4a standard [25], UWB systems are appropriate for a wide variety of specific WSN applications. These applications include locating and imaging of objects and environments [15], perimeter intrusion detection [16], video surveillance [17], in-vehicle sensing [18], outdoor sports monitoring [27], monitoring of highways, bridges and other civil infrastructure [28] as common wireless sensor network technologies. It can be seen that UWB based WSN applications have been developed in numerous areas in industrial, governmental or military applications.

1.3. Contribution of the Thesis

Many previous studies in WSNs consider the detection of a primary user over a fading channel. Also, they consider the presence or absence of the primary user. That corresponds to one-bit decision. However, a primary user may be a dual-band system with uplink and downlink communication links. Therefore, two-bits (one for uplink, and one for downlink) may be assessed by sensors to decide on the absence or presence of the primary user. Furthermore, UWB based WSN is of main interest as it has many advantages as written earlier. In this work, we consider the implementation of distributed detection in IEEE 802.15.4a based wireless sensor networks in order to detect primary systems. Unlike earlier UWB based primary user detection studies which either perform detection using individual sensors, or which consider not-standardized UWB systems [26]-[30], we consider the standardized UWB based IEEE 802.15.4a systems in order to provide realistic detection results.

The system model of our study consists of two communication links. The first link was considered in [29], where the single user detection performance was assessed for uplink-downlink communications. Incorporation of the second link to the overall system will be the main focus and contribution of our work. Assuming a primary user with uplink-downlink communication links, each sensor will individually make a decision on the availability of the links (i.e., uplink and downlink) and will pass this information to the fusion center (FC) to obtain a more reliable decision. In the second link, the main factors that affect the detection performance are IEEE 802.15.4a specific signalling schemes (binary pulse position modulation (BPPM) vs. BPPM/binary phase shift keying (BPSK)), realistic IEEE 802.15.4a channel models and the signal-to-noise-ratio (SNR), and the fusion rule at the FC. In addition, the number of sensors and the transmission rate will also affect the system performance. In this thesis, we:

1. implement the multiple sensor network, and consider various receiver structures,
2. obtain the probability of false alarm and detection expressions, and also the probabil-

ities for all possible outcomes according to absence of the primary user,

3. transmit the decision of each sensor about the primary user with either noncoherent binary pulse position modulation (BPPM) or coherent BPPM-binary phase shift keying (BPPM/BPSK) modulation, and
4. derive the mathematical expressions to quantify the probability of error for noncoherent signalling in the second link in addition to simulation based studies.

These main contributions are presented in Chapters 3 and 4. The results are important for the implementation of primary user detection in IEEE 802.15.4a based WSNs.

1.4. Organization of the Thesis

The rest of the thesis is organized as follows. In Chapter 2, UWB-based WSNs are presented. In Chapter 3, IEEE 802.15.4a based signalling with two different modulation formats are presented. In Chapter 4, non-coherent receiver structure and the second-link performance analysis are presented. In both Chapters 3 and 4, numerical and simulation results are presented for the comparison of the considered modulations and receiver structures under various scenarios. Concluding remarks and possible future research directions are given in Chapter 5.

2. UWB BASED WSNs

Ultra wideband (UWB) systems are among the most attractive technologies which provide some crucial requirements, such as low energy consumption and low complexity, for wireless sensor networks (WSNs). The system model to be used in the detection of a primary user with UWB based WSN, consists of two communication links as shown in Fig. 2.1 In the first, link which is the link between the primary user and the sensors, each sensor makes a decision to determine the availability of uplink-downlink communication links of the primary user. Sensors make their decisions by comparing the obtained energy with a predefined threshold. Hence, the availability information of the primary user $d_2 d_1 \in \{00, 01, 10, 11\}$ (0 represents the absence, 1 represents the presence) is decided as $\hat{d}_2^{(k)} \hat{d}_1^{(k)}$ at the kth sensor. In the second link, sensors transmit their decisions by using specific IEEE 802.15.4a signalling schemes, Binary Pulse Position Modulation (BPPM) or BPPM/Binary Phase Shift Keying (BPPM/BPSK), through the realistic IEEE 802.15.4a channel models to the fusion center (FC) to obtain a reliable decision. Fusion center gathers all the information and processes it according to a decision rule and makes a decision about the availability of uplink-downlink of primary user as $\hat{d}_2 \hat{d}_1 \in \{00, 01, 10, 11\}$. In this chapter, we present the primary user-sensor link structure and the sensor detection performance, consecutively.

2.1. Primary User - Sensor Link Structure

In the first link, which is the link between primary user and the sensor, sensors makes local decisions on the licensed user for both uplink and downlink, individually. These decisions are made according to two hypotheses, which represent the absence or the presence of

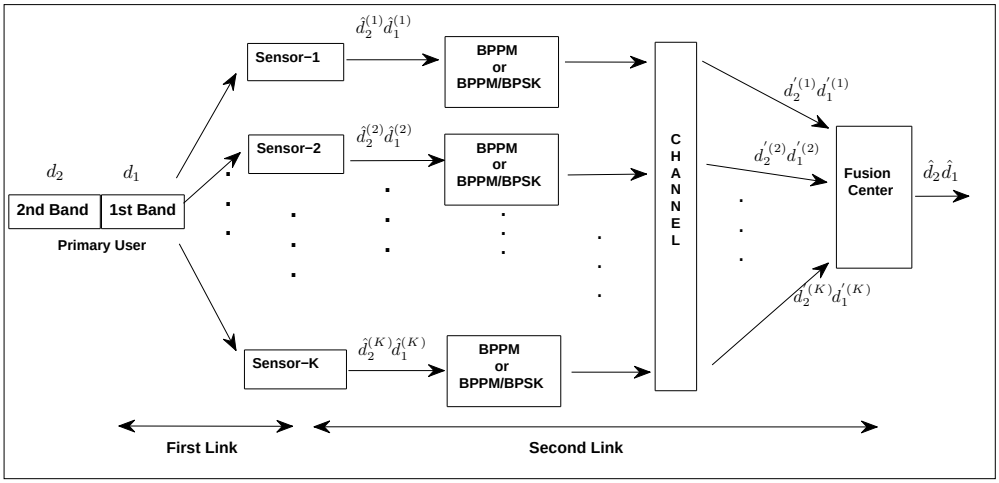

Figure 2.1. A UWB based WSN system

the primary user. The two hypotheses can be shown, respectively, for the mth link as:

$$H_{0,m}: \quad r_m(t) = n_m(t) \tag{2.1}$$

$$H_{1,m}: \quad r_m(t) = A_m\, e^{j\theta_m}\, s_m(t-\tau_m) + n_m(t) \tag{2.2}$$

where $r_m(t)$ is the received signal, $n_m(t)$ is band-limited additive white Gaussian noise (AWGN), and $s_m(t)$ represents the signal in the frequency band at that time with amplitude A_m and phase θ_m uniformly distributed over $[0, 2\pi)$, and τ_m is the timing offset. In our system model, both links of the primary user are determined with this decision model, individually. In this model, d_2 and d_1 represent the uplink and downlink information, respectively. Considering this, possible cases can be denoted as $d_2 d_1 \in \{00, 01, 10, 11\}$. In [29], the Neyman-Pearson (NP) test was used to obtain the best detection performance for a desired false alarm rate. With this test, probability of detection is maximized by optimizing the threshold values $\{\lambda_m \mid m = 1, 2, ..., M\}$ jointly for a specific probability of false alarm $P_f = \alpha$. This can be shown as:

$$\begin{aligned} &\max_{\{\lambda_m \mid m=1,2,...,M\}} P_d \\ &s.t. \quad P_f = \alpha \end{aligned} \tag{2.3}$$

For our case, we assume $M = 2$ as it represents uplink and downlink. Next, we need to define P_f and P_d. In [29], both $d_2d_1 = 00$ (system is declared as passive) and $d_2d_1 \neq 00$ (system is declared as active) states were studied for one-sensor system. In this study, beyond the decision of absence or presence of the primary system made by each sensor, the overall detection performance is studied when the perceived 2-bit information are sent to the fusion center through the IEEE 802.15.4a channels. In this case, the probability of the decision as absent for both uplink and downlink of primary user by kth sensor can be shown for $j_{10} = (x_2x_1)_2$ situations as

$$P_j = \Pr[\hat{d}_2^{(k)}\hat{d}_1^{(k)} = 00 \mid d_2d_1 = x_2x_1] \tag{2.4}$$

where $j \in \{0, 1, 2, 3\}$ and $\hat{d}_2^{(k)}\hat{d}_1^{(k)}$ is the decision of kth sensor about the primary user. As in [29], in the case that there is one sensor in the system, the probability of false alarm and the probability of detection can be written as

$$P_f = 1 - P_0 \tag{2.5}$$

$$P_d = \sum_{j=1}^{3} \frac{\Pr[d_2d_1 = x_2x_1]}{1 - \Pr[d_2d_1 = 00]}(1 - P_j). \tag{2.6}$$

2.2. Sensor Detection Performance

In the first link, an energy detection based spectrum sensing model is used to determine the absence or the presence of the primary user at each sensor. This model indicates two hypotheses given in (2.1) and (2.2), representing the two different cases of the primary user [29]. Accordingly, a decision variable defined for the mth system by using a square-law detector as

$$d_m = \frac{2}{N_0} \int_0^{T_m} |r_m(t)|^2 \, dt \tag{2.7}$$

where T_m is the integration time for the mth system and $|\cdot|$ is the absolute value operator. Assuming that the signal samples also have zero-mean Gaussian distribution, the probability density function (pdf) of d_m for both situations can be expressed as [29]

$$f_{D_m}(d_m) = \frac{1}{\sigma_m^{N_m} \, 2^{N_m/2} \, \Gamma(N_m/2)} \, d_m^{N_m/2-1} e^{-d_m/2\sigma_m^2}. \tag{2.8}$$

For a passive system, the variance term is $\sigma_m^2 = \frac{\sigma_{nm}^2}{N_0 W_m} = 1$, but for an active system, the variance term is $\sigma_m^2 = \gamma_m + 1$, where the SNR is defined as $\gamma_m = \frac{A_m^2 \sigma_s^2}{N_0 W_m}$ with σ_s^2 being the variance of the primary signal samples [29]. $N_m = 2T_m W_m$ is the degree of freedom, where W_m is the bandwidth of the bandlimited signal. In the first link, the detection is made by comparing the decision variable with a predefined threshold value λ_m for the mth system ($m = 1$, downlink; $m = 2$, uplink). The probabilities of misdetection P_{md} and false alarm P_f are two key parameters of spectrum sensing. The probability of misdetection is the probability that a secondary system can not detect the primary system when the primary system is active and this causes interference to the primary system. On the other hand, the probability of false alarm is the probability that the sensor decides on the presence of a primary user when there is no active primary system. The probability false alarm gives information about how efficiently the frequency band can be used while the primary user is not active in the system. The probability of misdetection also gives information about how well coexistence may occur in that frequency band. Probability of false alarm and probability of detection for the mth band can be given as

$$P_{f,m} = \Pr[d_m > \lambda_m | H_{0,m}] \tag{2.9}$$

$$P_{d,m} = \Pr[d_m > \lambda_m | H_{1,m}]. \tag{2.10}$$

The probabilities of false alarm and misdetection for the mth band of the primary user, can be written by using regularized upper incomplete Gamma function as [29]

$$P_{x,m} = Q\left(\frac{N_m}{2}, \frac{\lambda_m}{2\sigma_m^2}\right) = \frac{\Gamma\left(\frac{N_m}{2}, \frac{\lambda_m}{2\sigma_m^2}\right)}{\Gamma\left(\frac{N_m}{2}\right)}, \ x \in \{f, d\}. \tag{2.11}$$

In this thesis, the main contribution is the investigation of the sensor-fusion center link. On the other hand, the single sensor detection performance presented in this chapter will be incorparated into the overall system performance. In Chapters 3 and 4, the sensor-fusion center link will be investigated in detail. Next, the effect of IEEE802.15.4a modulations on the detection performance is presented.

3. IEEE 802.15.4a SIGNALLING

Many different signalling schemes are developed in wireless sensor networks to enhance the primary user detection performance. In the same manner, IEEE 802.15.4a standard is developed by the IEEE standardization group to obtain a physical layer for sensor network applications, in 2007. This standard has the ability to support multiple users to provide efficient spectrum usage within a single frequency band. In addition, IEEE 802.15.4a standard adopts UWB-IR for its physical layer to obtain reliable and robust data transmissions and ranging accuracy. Due to these aspects, IEEE 802.15.4a standard uses specific modulation types, coding and ranging waveforms with either coherent or non-coherent receivers [25]. In this chapter, two different IEEE 802.15.4a signalling schemes are investigated for various false alarm and misdetection cases of the first link.

In the second link, IEEE 802.15.4a based modulations and channel models are used to transmit the information. The structure of the modulations in IEEE 802.15.4a are based on time-hopping impulse radio (TH-IR) which was introduced in 1993 by Scholtz [31] and better utilized by Win and Scholtz [23],[32]. In TH-IR, a sequence of pulses with various delays represents each data symbol and this pulse sequence is applied to modulation. In these modulations, the multipath components of the short pulses need to be properly received and processed [21]. Each sensor sends the decision $\hat{d}_2^{(k)}\hat{d}_1^{(k)}$ with the specific IEEE 802.15.4a modulations, BPPM or BPPM/BPSK, to the fusion center.

3.1. Double Duration - Binary Pulse Position Modulation (DD-BPPM)

In classical approach of BPPM, the availability of the primary user is decided and transmitted by each sensor as 0 when both uplink and downlink are passive, and is decided and transmitted as 1 when at least one of the links is active. Due to this approach, the 0 (passive) information is positioned on the first half of the T_s, signal duration, and 1 (active)

is positioned on the second half of the T_s as shown in Fig. 3.1.

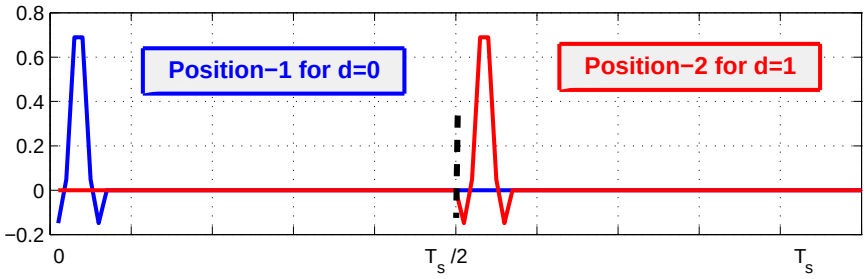

Figure 3.1. Illustration of a BPPM signal transmission

In this study, each sensor decision is used as 2-bit information, one of them carrying information about uplink, the other one carrying the information about downlink. Each sensor sends this information to the fusion center individually. In this circumstance, the information is sent in $2T_s$ (double) duration for one sensor as illustrated in Fig. 3.2.

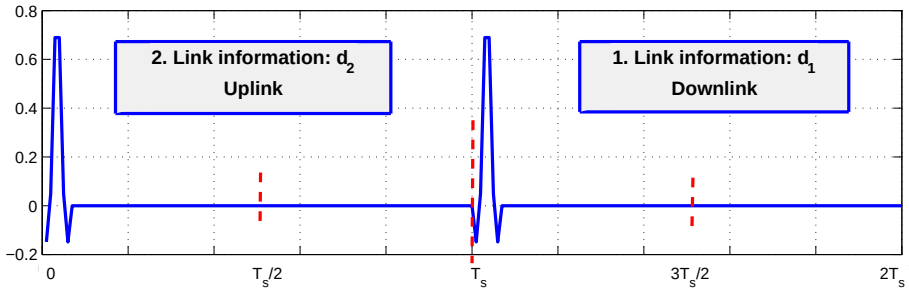

Figure 3.2. Illustration of a DD-BPPM signal transmission

The BPPM received signal can be represented mathematically as

$$r^{(k)}(t) = w^{(k)}(t) * h^{(k)}(t) + n^{(k)}(t) \tag{3.1}$$

where $n^{(k)}(t)$ is white Gaussian noise, $w^{(k)}(t)$ is the symbol of the $\hat{d}_m^{(k)}$ information which is decided by the kth sensor and represented as

$$w^{(k)}(t) = p\Big(t - \hat{d}_m^{(k)} \frac{T_s}{2}\Big) \tag{3.2}$$

where $p(t)$ is the transmitted pulse. $h^{(k)}(t)$ represents IEEE 802.15.4a channels and can be shown as

$$h^{(k)}(t) = \sum_{i=0}^{L-1} h_i \delta(t - \tau_i) \tag{3.3}$$

where h_i is the ith multipath coefficient, τ_i is the ith components of the multipath delay, L is the number of components of the multipath delay, and $\delta(.)$ is the Dirac delta function. More details on the channel model are provided in the Appendix.

At the receiver side, the received signal $r^{(k)}(t)$ is processed to decide on the transmitted data. BPPM data can be recovered noncoherently where it is preferred for its energy efficient structure in WSNs. For noncoherent modulations, energy detection method is the most common method. In this study, the integration duration to gather the energy of the received signal is $T_i < (T_s/2)$. In this case, the integration range of the first position is $[0, T_i]$ and the integration range of the second position is $[T_s/2, (T_s/2 + T_i)]$. The gathered energies for both positions are calculated as

$$R_{m,l}^{(k)} = \int_{l\frac{T_s}{2}}^{l\frac{T_s}{2}+T_i} |r^{(k)}(t)|^2 \, dt, \quad l = \{0, 1\}. \tag{3.4}$$

The decision for the received local observations of each sensor at the fusion center, $d_m^{\prime(k)}$, are decided by comparing the energies of the positions ($m \in \{1, 2\}$) with each other:

$$d_m^{\prime(k)} = \begin{cases} 0 & ; R_{m,0}^{(k)} > R_{m,1}^{(k)} \\ 1 & ; \text{otherwise} \end{cases} \tag{3.5}$$

3.2. BPPM/Binary Phase Shift Keying (BPPM/BPSK)

BPPM/BPSK is a hybrid modulation which is a combination of BPPM and BPSK modulations. In this modulation, while one link information is sent as position information, the other link information is sent as the phase information by each sensor. Transmission of each link information is depicted as shown in Fig. 3.3.

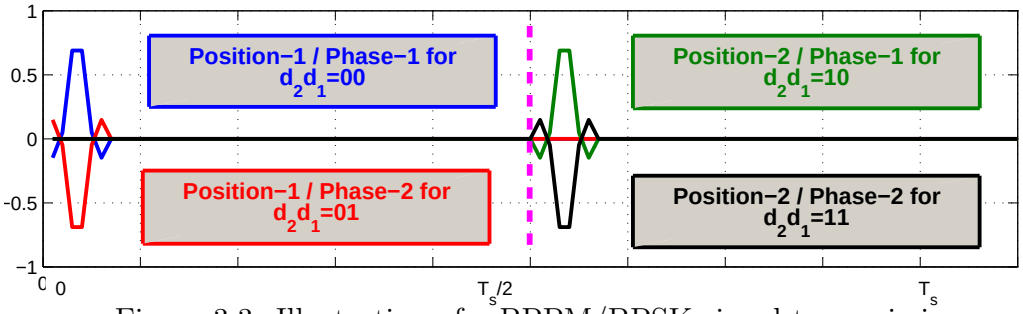

Figure 3.3. Illustration of a BPPM/BPSK signal transmission

The signal to be transmitted can be obtained by using both uplink-downlink information as

$$w^{(k)}(t) = \hat{d}_{c,k}^{(k)} p\Big(t - \hat{d}_2^{(k)} \frac{T_s}{2}\Big) \tag{3.6}$$

where $\hat{d}_{c,k}^{(k)}$ is the phase information which converts the information of $\hat{d}_1^{(k)} \in \{0, 1\}$ to $\{\pm 1\}$ phase information. The received signal has the same structure as given in (3.1):

$$r^{(k)}(t) = w^{(k)}(t) * h^{(k)}(t) + n^{(k)}(t) \tag{3.7}$$

At the receiver side, the 2-bit data can be recovered coherently in the case of channel coefficients are being estimated. A coherent receiver needs to use rake receivers, where the

correlation receiver output is given as

$$R_{i,m}^{(k)} = \int_{-\infty}^{\infty} r(t) v_m(t - \tau_i) dt, \quad i \in \{0, ..., L_r - 1\} \tag{3.8}$$

where L_r is the number of rake fingers and $v_m(t)$ is the reference signal

$$v_m(t) = p\Big(t - m\frac{T_s}{2}\Big), m \in \{0, 1\}. \tag{3.9}$$

The output of each correlation can be combined to give the decision variable as

$$R_m^{(k)} = \sum_{i=0}^{L_r - 1} h_i^{(k)} R_{i,m}^{(k)} \tag{3.10}$$

where $\{R_m^{(k)}\}$ carries both the position and phase information. Therefore, the decisions about links, $d_2^{'(k)} d_1^{'(k)}$, can be obtained as

$$\begin{aligned} \max\{|R_m^{(k)}|\} = R_{d_2^{'(k)}}^{(k)} \rightarrow \quad & d_2^{'(k)} \\ \text{sign}\{R_{d_2^{'(k)}}^{(k)}\} \rightarrow \quad & d_1^{'(k)}. \end{aligned} \tag{3.11}$$

3.3. Fusion Center

The observation data, which comes from each sensor, are gathered at the fusion center and the fusion center makes a global decision about the primary user by using the majority rule. In the case when only one sensor is active in the system, there is no need to use the majority rule. Majority rule is applicable for the case when at least two sensors are active in the system. For the multi-sensored systems, it is assumed that each sensor transmits its local decision to the fusion center through orthogonal channels. In the first link, probabilities

of false alarm and misdetection are calculated using (2.9) and (2.10), respectively. In the second link, likewise the probabilities of false alarm and misdetection of the first link, the probability of error is calculated for each bit transmitted as

$$P_{e,m} = \Pr[d_m^{'(k)} \neq \hat{d}_m^{(k)} \mid \hat{d}_m^{(k)} = x_m], \qquad x_m \in \{0, 1\} \tag{3.12}$$

where m is equal to 1 for downlink, and 2 for uplink. Based on the information that comes from the first channel, the probability of both uplink and downlink being decided as passive by the fusion center for the possible four different j cases, where $j \in \{0, 1, 2, 3\}$, can be shown as

$$P_{e,j} = \prod_{m=1}^{2} (P_{e,m})^{x_m^{(k)}} (1 - P_{e,m})^{(1-x_m^{(k)})}. \tag{3.13}$$

3.3.1. One-sensor active

When there is only one sensor active in the system, fusion center makes a decision with respect to $\{d_2^{'(k)} d_1^{'(k)}\}$ information. Hence, the probability of false alarm, $P_{f,T}^{(k)}$, and misdetection, $P_{md,T}^{(k)}$, for the overall system, can be obtained as

$$P_{f,T}^{(k)} = \sum_{j=0}^{3} P_{p,j} \, (1 - P_{e,j}) \tag{3.14}$$

and

$$P_{md,T}^{(k)} = \sum_{j=0}^{3} P_{a,j} \, (P_{e,j}) \tag{3.15}$$

where $P_{p,j}$ represents the probability of occuring four different j situations at the sensor when the primary user is passive, and $P_{a,j}$ is the probability of occuring four different j

situations at the sensor when the primary user is active, in (2.5) and (2.6), respectively.

3.3.2. Multi-sensored systems

All observations, which come from orthogonal channels are treated individually and decisions are made for each sensor. Fusion center decides an the absence/presence of the primary user by using the majority rule which is mostly preferred because of its low complexity structure. The majority rule is applied as:

$$D_m = \sum_{k=1}^{K} \{d_m^{'(k)}\}, \quad m = \{1, 2\} \tag{3.16}$$

$$\hat{d}_m = \begin{cases} 0 & \text{if } (D_m/K) < 0.5 \\ 1 & \text{if } (D_m/K) \geq 0.5 \end{cases} \tag{3.17}$$

The probability of false alarm, $\hat{P}_f$, and misdetection, $\hat{P}_{md}$, of the overall system can be obtained based on the final decision, $\hat{d}_m$, which is made by the fusion center:

$$\hat{P}_f = \Pr[\hat{d}_2\hat{d}_1 \neq 00 \mid d_2d_1 = 00] \tag{3.18}$$

$$\hat{P}_{md} = \Pr[\hat{d}_2\hat{d}_1 = 00 \mid d_2d_1 \neq 00] \tag{3.19}$$

3.4. Simulation Results

In this section, the effect of the probabilities of false alarm and misdetection of the first channel are investigated for three different situations as shown in Fig.3.4 [35]. The probability information of three cases are obtained from the study [29] by using the NP

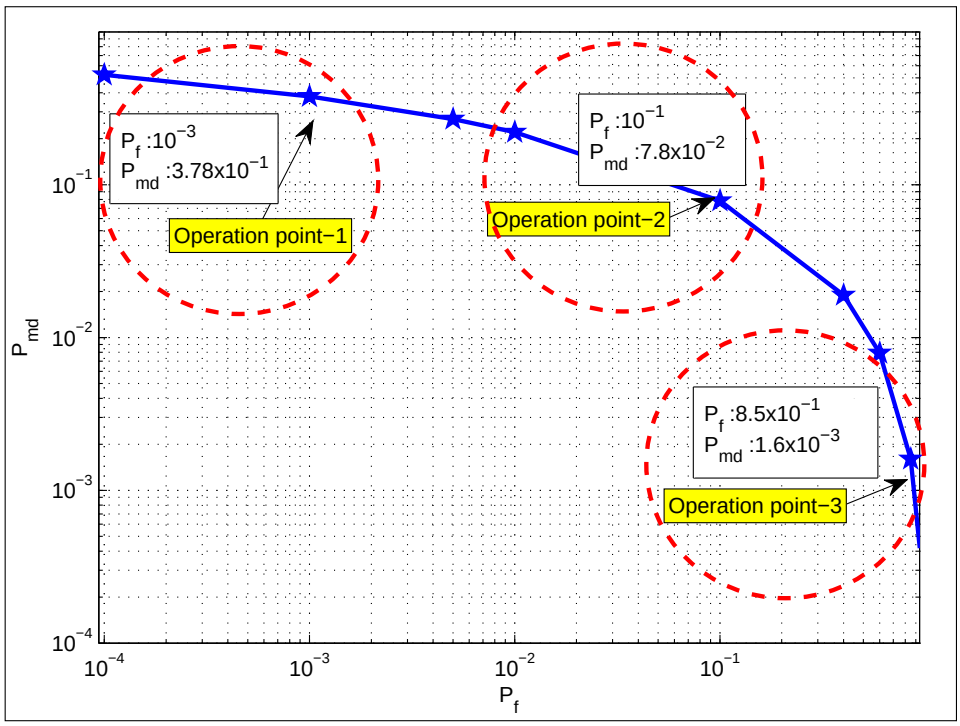

Figure 3.4. The operation points with probabilities, P_f and P_{md}, of the first channel

test for specific $P_f = \alpha$ values. In the first channel, the operation points are obtained when the SNR of both uplink and downlink are assumed as 5 dB. The information which is obtained on each operation point consists not only of the probabilities of false alarm and misdetection, but they also consist of the information for all possible j cases. The $P_{f,j}$ values that come from the first channel for each operation point 1, 2, and 3 are {0.9990, 0.00047, 0.00051, 0.00002}, {0.9, 0.0492, 0.0495, 0.0013}, {0.15, 0.3452, 0.3502, 0.1546}, and the $P_{md,j}$ values are {0.3784, 0.1899, 0.2814, 0.1503}, {0.0784, 0.1680, 0.4056, 0.3480}, {0.0016, 0.0964, 0.4509, 0.4511}, respectively. Operation points represent three distinct regions of $P_f - P_md$ trade-off. In the second channel, the residential line-of-sight, IEEE 802.15.4a channel model, CM1, is considered as the transmission channel. Results are obtained by using two different formats for various number of sensors $K = \{1, 4, 8, 16\}$.

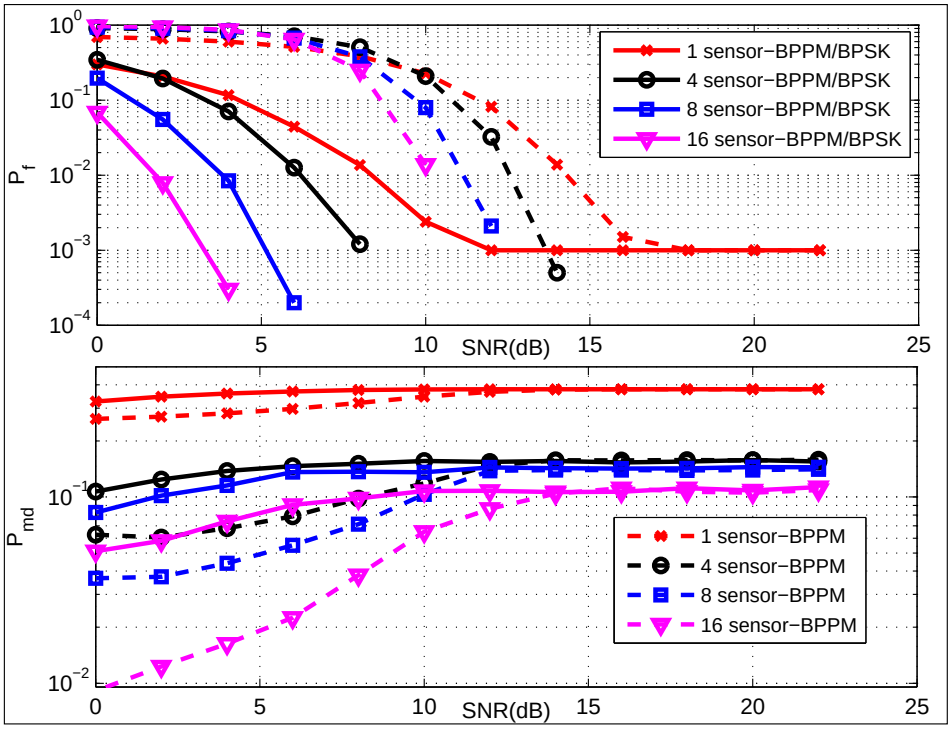

Figure 3.5. Overall performance for the 1st operation point

The simulation results are demonstrated in Fig. 3.5 for the operation point-1. In this scenario, the probability of false alarm for each sensor has lower values which means that the reliability of P_f is high for the first link. On the other hand, the probability of misdetection, P_{md}, values are high, meaning low reliability in the link for detection. In the case that there is only one sensor active in the system, the probability of causing interference to the primary user is very high. In the case that there is a multi-sensored system, the overall performance is evaluated for both P_f and P_{md} as the number of sensors increase. In low SNR region, BPPM/BPSK has a better performance than BPPM form the viewpoint of P_f while BPPM has better performance from the viewpoint of P_{md}. Hence, for the first point of operation, BPPM may be preferred for such a system that aims to protect the primary user.

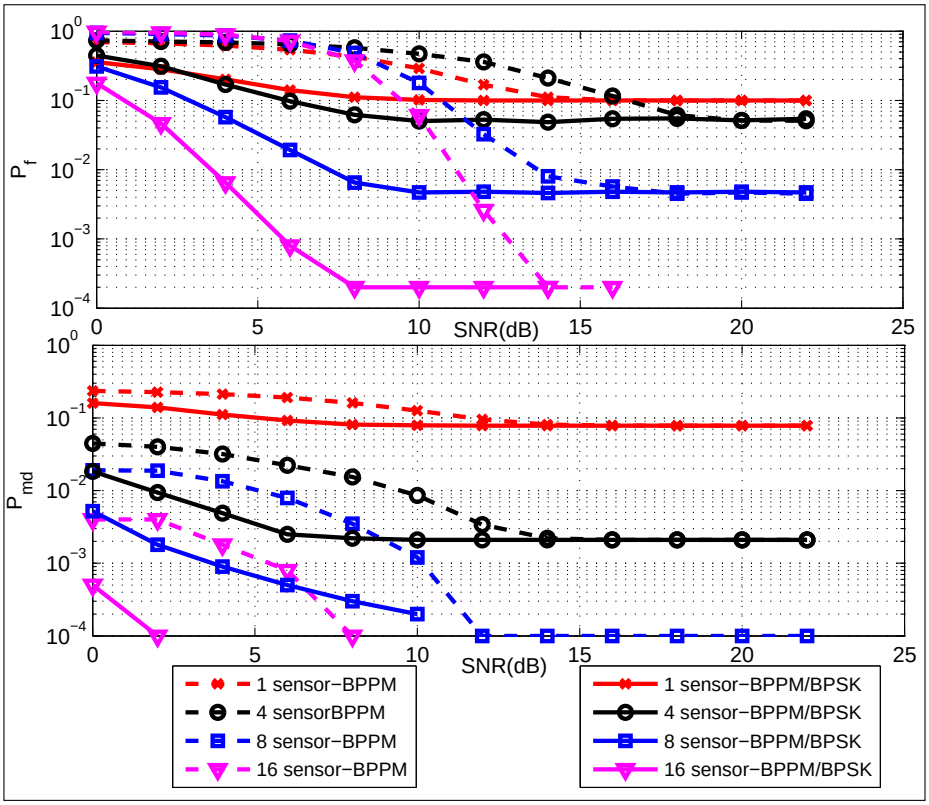

Figure 3.6. Overall performance for the 2nd operation point

As shown in Fig. 3.6, the second point of operation, where P_f is 0.1 and P_{md} is 0.078, both P_f and P_{md} enhance the performance better with BPPM/BPSK in the whole SNR range compared to BPPM. In this scenario, the frequency band can be used much more efficiently and primary user can communicate in a safer manner, at the same time.

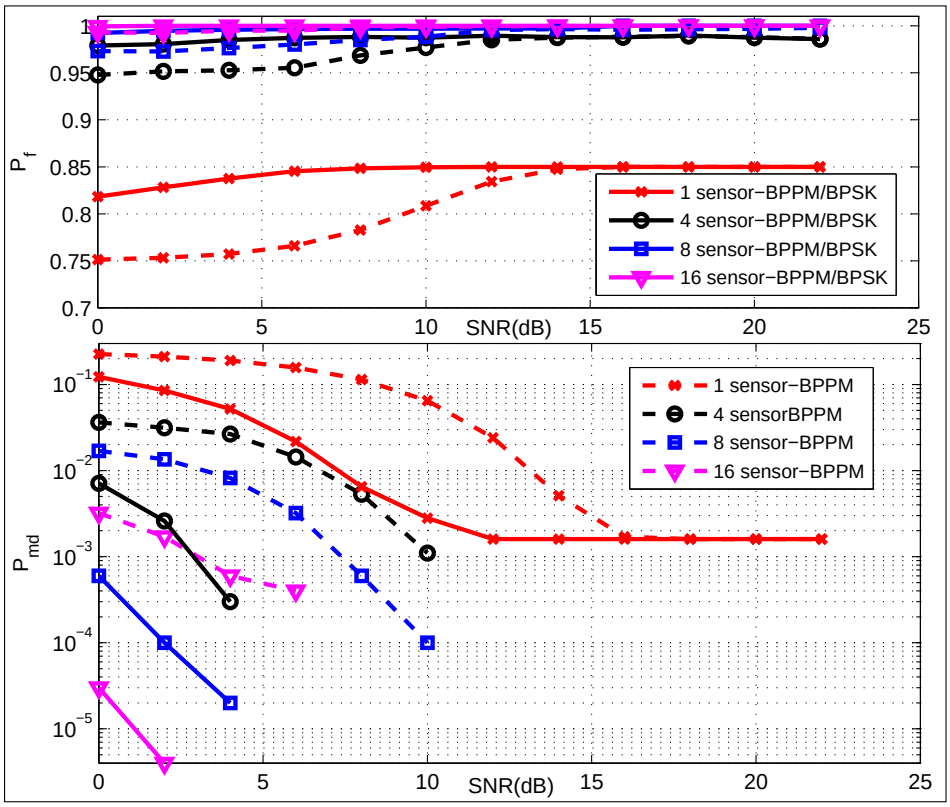

Figure 3.7. Overall performance for the 3rd operation point

Finally, the simulation results for the 3rd point of operation, when the reliability of P_f is low and P_{md} is high, are shown in Fig. 3.7. From the viewpoint of P_f, BPPM attains better performance in low SNR. As opposed to expected observations, the performance gets worse as the number of sensors increases. While more number of sensors are active in the wireless sensor network, the more amount of noisy data would be gathered and this results in decreasing the robustness of the decision. In this case, the frequency channel can not be used effectively when the primary user is passive in that channel. On the other hand, the performance of P_{md} of the overall system enhances especially with BPPM/BPSK modulation as the number of sensors increases. Hence, higher protection is provided for the primary users.

In this chapter, we studied the effects of IEEE 802.15.4a based signalling used in UWB based WSNs. When both P_f and P_{md} values are reasonably low, BPPM/BPSK performs

better as expected. On the other bound, it requires the knowledge of channel gains. However, a WSN should be both low-cost and energy-efficient. Therefore, in the next chapter we will further investigate UWB based WSNs that use BPPM and have noncoherent receiver structures.

4. NONCOHERENT RECEVER STRUCTURES FOR WSNs

In this chapter, we focus on noncoherent receiver structures for a specific method of data transmission. We investigate the performance of binary pulse position modulated signals while decreasing the energy consumption and complexity at the fusion center. The signals transmitted by each sensor are combined at the fusion center and a decision is made on the received signal. Accordingly, there is no need to use a complex fusion rule, as the fusion center only has to decide on the T_s duration received symbol. In Fig. 4.1, the noncoherent receiver structure is plotted. Sensors observe the primary user's activity, make local decisions

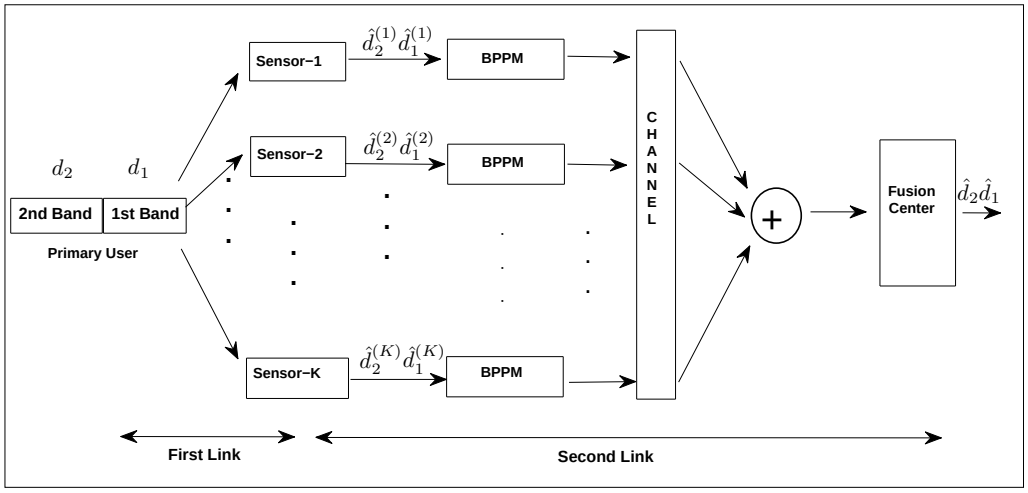

Figure 4.1. A UWB based WSN system with noncoherent receiver structure

and then transmit their decision to the fusion center using BPPM signalling. In the first channel, the absence/presence information is decided depending to the two hypotheses which are shown in (2.1) and (2.2). The details of probabilities of false alarm and misdetection of the first link (primary user-sensor link) were given in Chapter 2. In the second link the local active or passive decisions are gathered from sensors and transmitted to the fusion center.

4.1. System Model of the Sensor-Fusion Center Link

Binary pulse position modulation uses a constant amplitude and constant width signal, and position them according to the information of the primary user in wireless sensor networks. The BPPM received signal can be expressed as

$$r(t) = \sum_{k=1}^{K} s^{(k)}(t) * h^{(k)}(t) + n(t), \tag{4.1}$$

where $s^{(k)}(t)$ is the symbol of the $\hat{d}_m^{(k)}$ information (absent/present) of the kth sensor and is represented as

$$s^{(k)}(t) = p\left(t - d_m^{(k)}\frac{T_s}{2}\right), \tag{4.2}$$

and $n(t)$ is the AWGN with two-sided power spectral density $N_0/2$. While the UWB channel structure is complex and the power delay profile is in general double exponential decay model [37], it is not trivial to incorporate this model for analysis purposes. In this study, $h^{(k)}(t)$ represents channels as given in [26]

$$h^{(k)}(t) = \sum_{n=1}^{N} h_n^{(k)}\delta(t - nT_s), \tag{4.3}$$

where T_p is the channel resolution and the pulse duration, and $NT_p = T_s/2$ is the half-symbol duration. The channel coefficients are $\mathbf{h}^{(k)} = [h_1^{(k)} h_2^{(k)} ... h_N^{(k)}]$, where N is the length of channel coeffients. In practice, the double exponential decay model is used for the modeling of UWB channels in general [37], however, the Gaussian approximation model is used in this study as in [26]. Accordingly, each channel coefficient is assumed to be Gaussian distribution with $h_n^{(k)} \sim N(0, \sigma_h^2)$. At the receiver side, the energy detection method is used to determine the absence or the presence of the primary user. The instantaneous received energy, y_m, normalized by the noise power spectral density can be obtained easily for both two $m = \{0, 1\}$

positions as

$$y_m = \frac{2}{N_0} \int_{m\frac{T_s}{2}}^{(m+1)\frac{T_s}{2}} |r(t)|^2 dt. \tag{4.4}$$

The second step of the decision is the comparison of $\{y_m | m = 0, 1\}$ values. The energy values which are computed for the two positions separately are compared with each other for a decision. The position which has the maximum energy value is decided as the final decision of all sensors' combined observation. For analysis purposes, the discerete-time equivalent model to compute y_m can be written as

$$y_m = \frac{2}{N_0} \mathbf{r}_m^T \mathbf{r}_m, \tag{4.5}$$

where the $2N \times 1$ received vector $\mathbf{r}$ is concatenation of $N \times 1$ vectors $\mathbf{r}_0$ and $\mathbf{r}_1$, $\mathbf{r} = [\mathbf{r}_0 \mathbf{r}_1]$, given as

$$\mathbf{r}_m = \hat{d}_m \mathbf{S}\mathbf{h} + \mathbf{n}, \quad m = \{0, 1\}, \tag{4.6}$$

where $\mathbf{S}^{R \in (N \times N)}$ represents an $N \times N$ scalar matrix representing time-shifted pulses and $\mathbf{h}$ represents the combined effective channel for all K users. Since the elements of both $\mathbf{h}$ and $\mathbf{n}$ are Gaussian distributed, each element of $\mathbf{r}_m$ is zero mean and has a variance of $\sigma_{r_0}^2 = \sigma_h^2(K - i) + \sigma_n^2 K$ and $\sigma_{r_1}^2 = \sigma_h^2 i + \sigma_n^2 K$ for position "0" and position "1", respectively. Here, $i \leq K$ and $(K - i)$ represents the number of sensors transmitting "0" and "1", respectively. Therefore, y_m for positions $m = 0$ and $m = 1$ conditioned on i can be modelled with central χ^2-distribution with N degrees of freedom as in [29] and [38] by using (2.8) as

$$f_{Y_{0,K}}(y|i) = \frac{y^{N/2-1} e^{-y/2\{\sigma_h^2(K-i)+\sigma_n^2 K\}}}{\{\sigma_h^2(K - i) + \sigma_n^2 K\}^{N/2} 2^{N/2} \Gamma(N/2)} \tag{4.7}$$

$$f_{Y_{1,K}}(y|i) = \frac{y^{N/2-1}e^{-y/2\{\sigma_h^2 i+\sigma_n^2 K\}}}{\{\sigma_h^2 i+\sigma_n^2 K\}^{N/2}2^{N/2}\Gamma(N/2)} \tag{4.8}$$

where $\Gamma(.)$ is the gamma function defined in [39] as

$$\Gamma(p) = (p-1)!, \quad \text{when} \quad p > 0 \in Z. \tag{4.9}$$

In classical approach, a predefined treshold value is chosen and the final decision is given by using a comparison with this threshold [29], [38]. Therefore, obtaining an effective threshold is an optimization process which affects directly the performance of the system. In this study, the comparison between the gathered energies of the two positions can be used simply to make a decision when there are K sensors, and i out of K sensors decide "active" in the system. As an illustration, the pdf plots of the two positions are shown in Fig. 4.2 for the case that there are $K = 4$ sensors and the number of passive decisions is 3, (i.e., 3 sensors transmit at position-0 and 1 sensor transmits at position-1). Furthermore, without loss of generality, we assume that $d_m = 0$. Accordingly, depending on the detection performance of K sensors, each sensor transmits its decision to the FC. For the second link, there occurs an error if y_1 is greater than y_0. This can be shown as

$$P_e = \Pr[y_0 < y_1 \mid d_m = 0] = \Pr[\acute{y} < 0 \mid d_m = 0] \tag{4.10}$$

where $\acute{y} = y_0 - y_1$. Considering (4.7) and (4.8), the error probability can be numerically obtained by using the pdf of two positions. $\acute{y}$, the difference between the two central χ^2 distributions, can be calculated as the convolution of two pdfs as

$$P_{e|i} = \int_{-\infty}^{0} f_{y_0}(v|i) f_{y_1}((y+v)|i) dv. \tag{4.11}$$

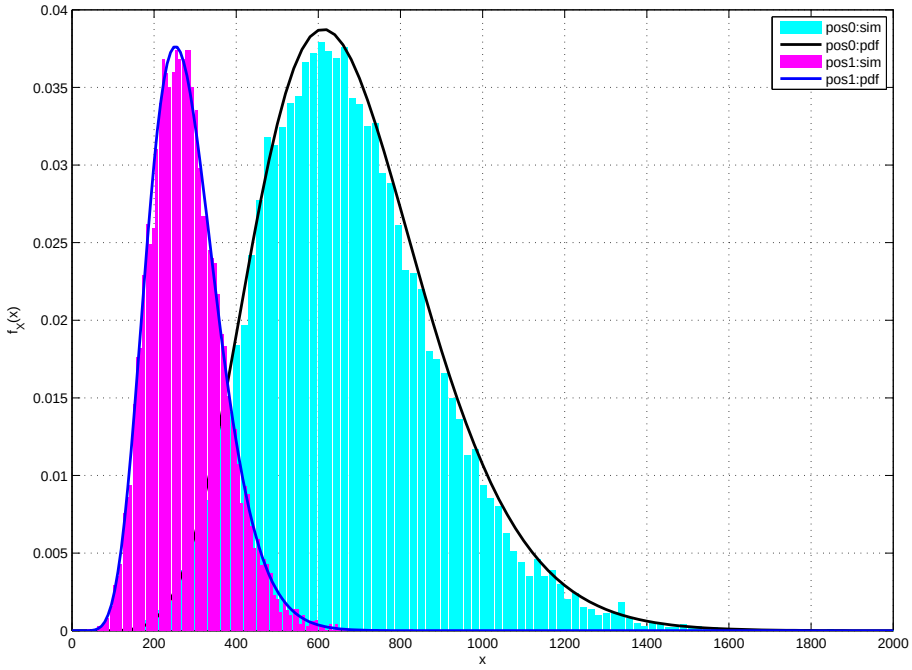

Figure 4.2. The pdfs of energy values obatained from two positions for 3 "passive" and 1 "active" decision for the 4 sensored case

The process of obtaining the probability of error can be illustrated as the convolution of the two energy distributions of the two positions. This is illustrated in Fig. 4.3 for a passive system being observed by $K = 3$ sensors, where $i = 0$ of them decide as active and $(K-i = 3)$ of them deicde as passive when the SNR of the second link is $SNR = 0dB$. Accordingly, the probaability of error can be obtained from this plot.

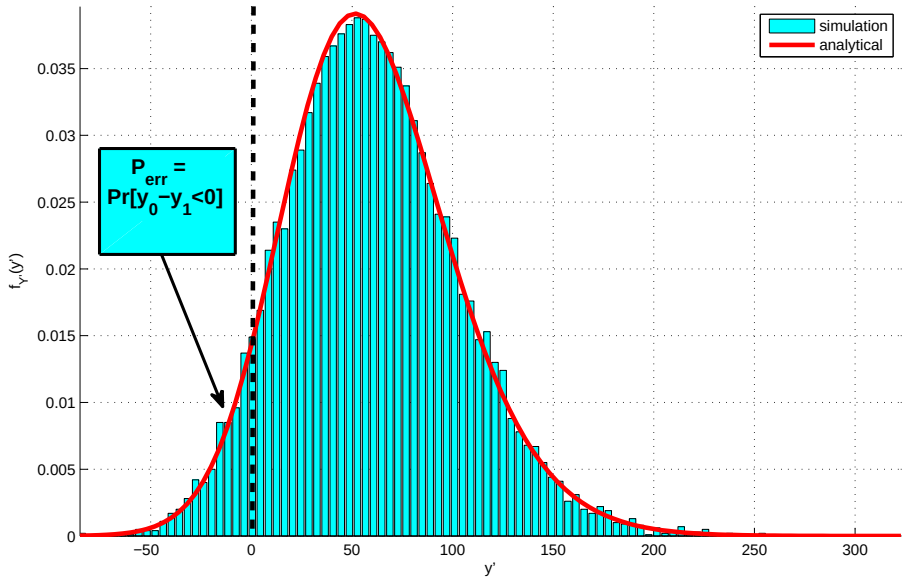

Figure 4.3. Probability of error for $K = 3$, and $i = 0$

4.2. Performance of the overall system

The probabilities of false alarm and detection expressions for the first link were obtained in Chapter 2. There are two possible decisions on the sensors "0"(absence) and "1" (presence). Each signal indicates two positions, $m \in \{0, 1\}$, therefore the number of possibilities are increased to 2^K, where K is the number of sensors. All the possibilities on the first channel can be obtained when $d_m = 0$ considering [38] as

$$P(i|H_0) = \begin{pmatrix} K \\ i \end{pmatrix} P_f^i (1 - P_f)^{(K-i)} \tag{4.12}$$

where P_f is the probability of false alarm of the first channel, which was explained in Chapter 2 and i is the number of active decisions on K sensors. Accordingly, the probability of error for the overall system can be obtained by using (4.11) and (4.12) including all i cases as

$$P_F = \sum_{i=0}^{K} P_{e|i}(i) P(i|H_0). \tag{4.13}$$

Similarly, following a similar approach of transmitting $d_m = 1$, instead of $d_m = 0$, P_D or P_{MD} can also be obtained. Next, we will present some numerical examples and confirm the validity of the model.

4.3. Results

After obtaining the necessary analytical expressions for the noncoherent system model, the validity of the system is confirmed with some numerical examples.Initially, the probability of error expression for the second link is validated, followed by the overall probability of false alarm performance. The system performance is tested for different number of sensors,where different number of users are active or passive. The length of the channel is $N = 20$ for all simulations and calculations. The calculated probability of error of the second channel is validated with the simulation of (4.10) and is illustrated in Fig. 4.4 for $K = \{1, 3, 5, 7\}$ sensors, which all decide passive. The probability of error of the second link tends to be 10^{-4} for 12 dB SNR when 7 sensors are active in the system, while it tends to be 10^{-1} when 1 sensor is active in the system for the same SNR value.

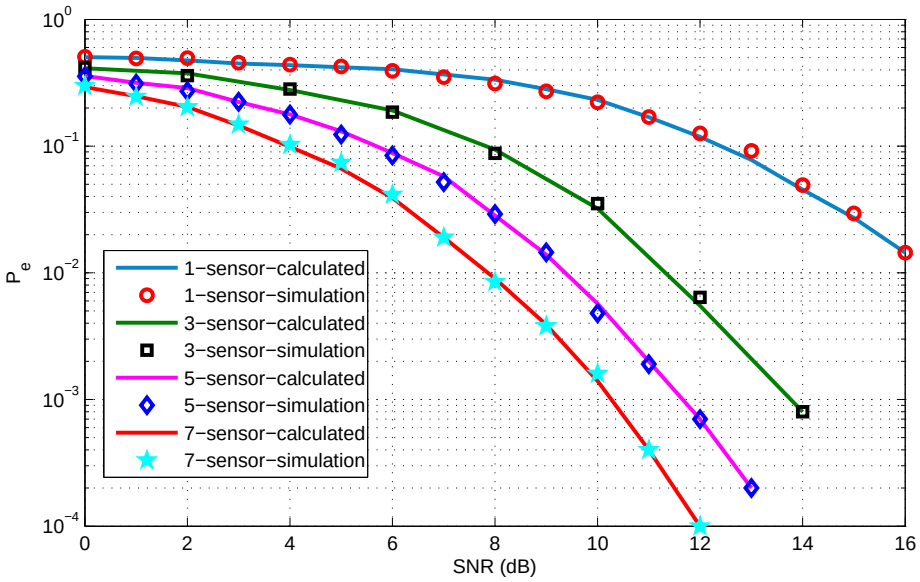

Figure 4.4. The probability of error for $K = \{1, 3, 5, 7\}$ sensors

In Fig. 4.5, different sensor cases are demonstrated for 3 sensors in the second link. There are four possibilities for 3 sensors from all active to all passive (all deciding "1" to all deciding "0"). The error calculation and simulation results are matched and are validated for various active sensors in the system. The performance of the system is enhanced as the same true decisions are increased.

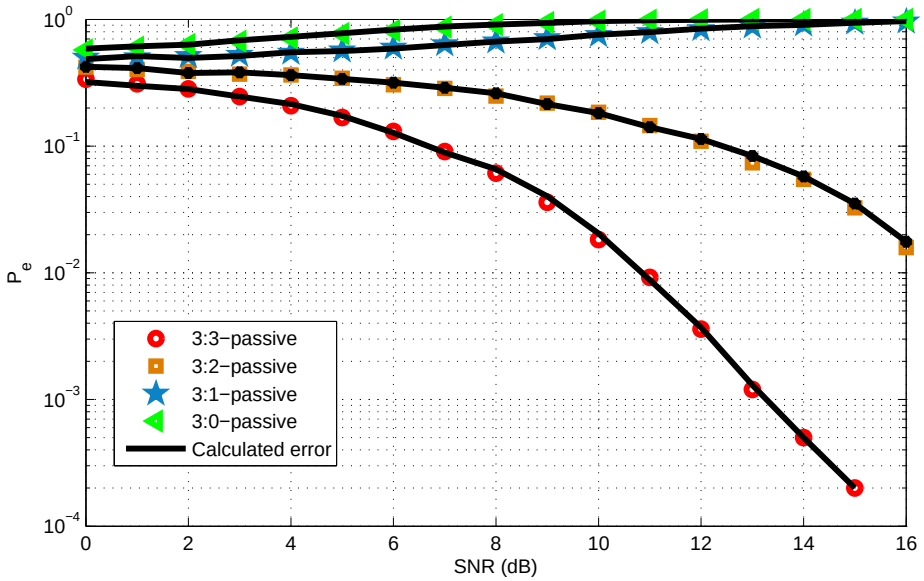

Figure 4.5. The probability of error for $K = 3$ and $i = \{0, 1, 2, 3\}$

Finally, the probability of false alarm of the overall system as given in (4.13) is presented in Fig. 4.6 for $K = \{1, 3, 5, 7\}$ sensors active in the system when the probability of false alarm of the first channel, P_f, is equal to 0.1. According to these results, the probability of false alarm, P_F, tends to be 10^{-4} when 15 sensors are active in the system, compared to a single-sensor achieving 10^{-1} for the same SNR value.

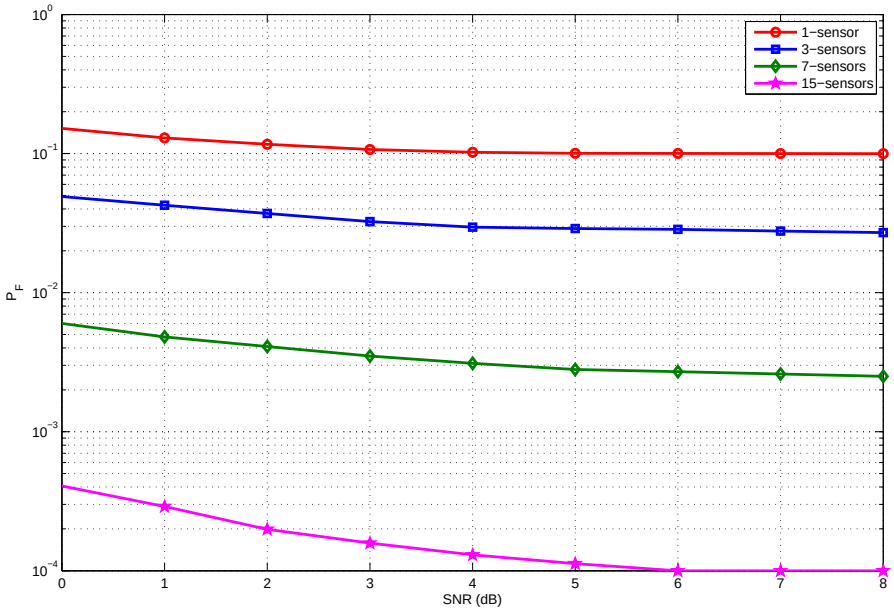

Figure 4.6. Probability of false alarm of the overall system when $P_f = 0.1$ for $K = \{1, 3, 7, 15\}$

5. CONCLUSIONS AND FUTURE RESEARCH

5.1. Conclusions

In this thesis, we investigated the primary user detection performance of UWB based WSNs and implemented IEEE 802.15.4a modulations for WSNs. Accordingly, various number of sensors make some observations for both links of the primary user. Afterwards, sensors transmit their observations to a fusion center that has two different IEEE 802.15.4a receiving structures, coherent and non-coherent, through the realistic IEEE 802.15.4a channels. In UWB based WSNs:

- Uplink/downlink observations are transmitted individually rather then a single decision for both link.
- The performances of two different modulations, DD-BPPM and BPPM/BPSK, are investigated for various situations of the first channel.
- A non-coherent modulation may have better performance than a coherent one under low SNR for some specific situations of the first channel.
- When the reliability of P_f or P_{md} of the first channel is low, BPPM enhances the performance better than BPPM/BPSK. However, BPPM/BPSK still provides better performance for other situations.
- In some case of the first channel, the increase on the number of sensors can decrease the performance as a result of gathering more noise with each sensor.
- In Chapter 4, the noncoherent receiver structure with BPPM signals were investigated in detail and the simulation results are supported with theoretical calculations. The performance of the system increased with number of sensors.

5.2. Future Research

The thesis focused on spectrum sensing of UWB based WSNs when all the joint activity values were fixed and the positions of the sensors were incorparated into the system model. Future work many include the effects of positions of the sensors in a network and the effects of joint activity values.

APPENDIX A: IEEE 802.15.4a Channels

UWB channel models (CMs) are developed in the IEEE 802.15.4a standard. In this study, CM-1, residental line-of-sight model, is considered as the second channel (i.e, sensor-fusion center channel). This channel model covers the range of 0-4m. The parameters of CM-1 and the details can be found in [34] and [37]. CM1 represents a residential line-of sight (LOS) scenario. The IEEE 802.15.4a channels, $h^{(k)}(t)$, can be represented as

$$h^{(k)}(t) = \sum_{i=0}^{L-1} h_i \delta(t - \tau_i) \tag{A.1}$$

where h_i, τ_i, L and $\delta(.)$ are the ith multipath channel coefficient, ith multipath component delay, number of multipath components and Dirac delta function, respectively. A single channel realization of CM1 is plotted in Fig. A.1 for a channel resolution of 1ns.

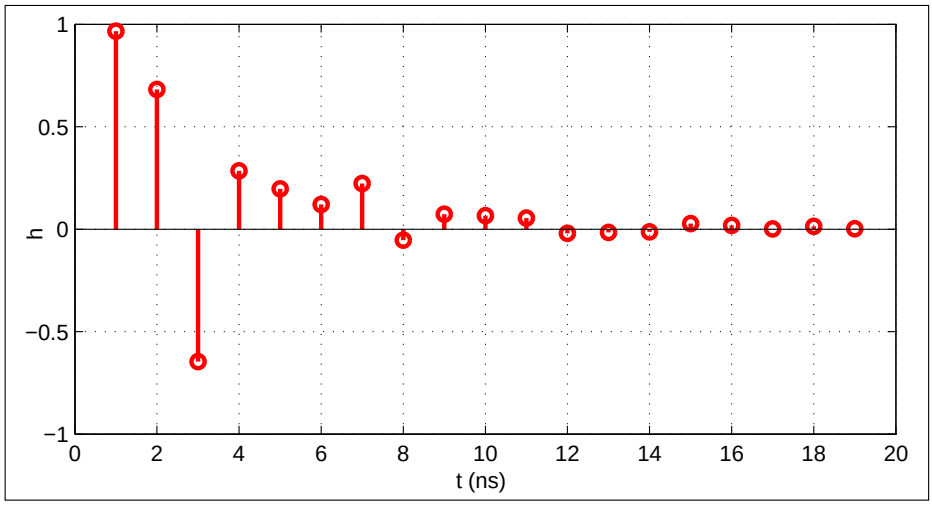

Figure A.1. Illustration of IEEE 802.15.4a Channel Model 1

REFERENCES

1. B. Liu and B. Chen, "Channel-optimized quantizers for decentralized detection in sensor networks," *IEEE Trans. Info. Theory*, vol. 52, pp. 33–49, July 2006.

2. R. Jiang and B. Chen, "Fusion of censored decisions in WSNs," *IEEE Trans Wireless Commun.*, vol. 4, pp. 2668–2673, Nov. 2005.

3. A. Mechodniya, et. al., "Distributed detection in UWB sensor networks under non-orthogonal Nakagami-m fading," *IEEE Proc. VTC-Fall*, pp. 1–5, 2011.

4. K. Liu and A. M. Sayeed, "Type-based decentralized detection in wireless sensor networks," *IEEE Trans Sig. Proc.*, vol. 55, pp. 1–5, May. 207.

5. S. Kumar, F. Zhao, D. Shepherd (Eds.), Special issue on collaborative signal and information operationing in microsensor networks, *IEEE Signal Proc. Mag.*, 2002.

6. H. Gharavi, S. Kumar (Eds.), Special issue on sensor Networks and applications, *IEEE Proc.*, 2003.

7. A. Sayeed, D. Estrin, G. Pottie, K. Ramchandran (Eds.), Self-organizing distributed collaborative sensor networks, *IEEE J. Select. Commun.*, 2005.

8. Z. Chair, P.K. Varshney, Optimal data fusion in multiple sensor detection systems, *IEEE Trans. Aerospace Electron. Syst.*, pp. 98-101, 1986.

9. P. K. Varshney, Distributed Detection and Data Fusion, *Springer*, New York, 1997.

10. R. Niu, P. K. Varshney, Q. Cheng, Distributed detection in a large wireless sensor net-

work, *Seventh International Conf. on Information Fusion*, 2005

11. P.K. Willett, P.F. Swaszek, R.S. Blum, The good, bad, and ugly: distributed detection of a known signal in dependent Gaussian noise,*IEEE Trans. Signal Proc.*,pp. 3266-3279, 2000.

12. E. Drakopoulos, C.C. Lee, Optimum multisensor fusion of correlated local decisions,*IEEE Trans. Aerospace Electon. Syst.*, pp. 593-605, 1991.

13. M. Kam, W. Chang, Q. Zhu, Hardware complexity of binary distributed detection systems with isolated local Bayesian detectors, *IEEE Trans. Systems Man Cybernet*, pp. 565-571, 1991.

14. M. Kam, Q. Zhu, W.S. Gray, Optimal data fusion of correlated local decisions in multiple sensor detection systems,*IEEE Trans. Aerospace Electon. Syst.*, pp. 916-920, 1992.

15. R.S. Thoma, O. Hirsch, J. Sachs, R. Zetik, UWB sensor networks for position location and imaging of objects and environments,*The Second European Conference on Antennas and Propagation (EuCAP)*, pp. 1–9, 2007.

16. L. Yuheng, L. Chao, Y. He, J. Wu, Z. Xiong, A Perimeter intrusion detection system using dual-mode wireless sensor networks,*Second International Conference on Communications and Networking*, pp. 861–865, 2007.

17. X. Huang, E. Dutkiewicz, R. Gandia, D. Lowe, Ultra-wideband technology for video surveillance sensor networks,*IEEE International Conference on Industrial Informatics*, pp. 1012–1017, 2006.

18. J. Li, T. Talty, Channel characterization for ultra-wideband intra-vehicle sensor Networks, Military Communications conference (MILCOM), pp. 1–5, 2006.

19. F. Granelli, H. Zhang, X. Zhou, S. Maran, Research advances in cognitive ultra wide band radio and their application to sensor networks,*Mobile Networks and Applications*, Vol. 11, pp. 487–499, 2006.

20. L. Stoica, A. Rabbachin, H.O. Repo, T.S. Tiuraniemi, I. Oppermann, An ultra wideband system architecture for tag based wireless sensor networks, *IEEE Transactions on Vehicular Technology*, Vol. 54, pp. 1632–1645, 2005.

21. J. Zhang, P. Orlik, Z. Şahinoğlu, A. Molisch, P. Kinney, UWB systems for wireless sensor networks, *IEEE Proc., Mitsubishi Electric Research Laboratories*, Vol. 97, No. 2, February 2009,

22. J. Mitola and G. Q. Maguire, Cognitive radio: making software radios more personal, *IEEE Personal Commun.*,vol.6, pp.13–18, 1999.

23. M. Z. Win and R. A. Scholtz, Ultra-wide bandwidth time-hopping spread-spectrum impulse radio for wireless multiple-access communications, *IEEE Trans. Commun.*, vol.48, pp.679–691, 2000.

24. F. Li, J. S. Evans, and S. Dey, Decision fusion over noncoherent fading multiaccess channels, *IEEE Trans. Signal Proc.*, vol. 59, pp. 4367–4380, Sept. 2011.

25. Amendment to IEEE Std. 802.15.4,*IEEE Std. 802.15.4a-2007, IEEE Computer Society*, 2007.

26. K. Bai and C. Tepedelenlioğlu, Distributed detection in UWB wireless sensor networks, *IEEE Trans. Signal Proc.*, vol. 58, pp. 804–813, Feb. 2010.

27. I. Oppenmann, L. Stoica, A. Rabbachin, Z. Shekby, and J. Haapola, UWB wireless sensor networks: UWENVA practical example, *IEEE Commun. Mag.*, pp. 27-32, 2004

28. V. Mehta and M. EI Zarki, An ultra wide band (UWB) based sensor network for civil infrastructure health monitoring, *Proc. 1st Eur. Workshop Wireless Sensor Netw. (EWSN)*, Germany, 2004.

29. S. Erküçük, L. Lampe, and R. Schober, Joint detection of primary systems using UWB impulse radios, *IEEE Trans. Wireless Commun.*, vol. 10, pp. 419–424, Feb. 2011.

30. T. Hozumi, M. Fujii, and Y. Watanabe, A Study on cooperative interference detection for UWB systems, *IEEE Proc. ICUWB*, pp. 76–80, 2011.

31. R.A. Scholtz, Multiple access with time-hopping impulse modulation, *Proc. Milcom*, Oct. 1993.

32. M. Z. Win and R. A. Scholtz, Impulse radio: How it works, *IEEE Commun. Lett.*, vol. 2, pp. 36-38, Feb. 1998.

33. F. Cuomo, C. Martello, A. Baiocchi, and C. Fabrizio, Radio resource sharing for ad-hoc networking with UWB, *IEEE J. Sel. Areas Commun.*, vol. 20, pp. 1722-1732, Dec. 2002.

34. J. R. Foerster, M. Pendergrass, A. F. Molisch, A Channel model for ultra wideband indoor communication, *Mitsubishi Electric Research Laboratories*, TR2004-074, 2003

35. Y. Sabucu , S. Erküçük, Primary user detection IEEE 802.15.4a based wireless sensor networks, *IEEE Signal Proc. SIU.*, 2013

36. K. Witrisal, G. Leus, G.J.M. Janssen, M. Pausini, F. Troesch, T. Zasowski, and J. Romme, Noncoherent ultra-wideband systems, *IEEE Signal Proc. Magazine*, pp. 48–66, July, 2009

37. A. F. Molisch, K. Balakrishnan,and et al., IEEE 802.15.4a channel model, *IEEE Std.*,

2007

38. S. Yiu, R. Schober, Nonorthogonal Transmission and Noncoherent Fusion of Censored Decisions, *IEEE Trans. Veh. Technol.*, vol. 58, pp. 263-273, Jan. 2009.

39. J. G. Proakis, Digital Communications, *4th edition*, McGraw Hill, 2000.

Curriculum Vitae

Yağmur Sabucu was born on 11 August 1989, in Eskişehir. She received her BSc degree in Electronics Engineering in 2011 from Kadir Has University. She worked as a research assistant in the 7^{th} European Community Framework Programme - Marie Curie International Reintegration Grant project and worked as teaching assistant at the Department of Electronics Engineering of Kadir Has University from 2011 to 2013. Her research interests include UWB systems and wireless sensor networks.

Publications:

* Y. Sabucu and S. Erküçük, Primary user detection in IEEE 802.15.4a based wireless sensor networks, IEEE Signal Proc. Appl. Conf., KKTC, pp. 1 - 4, April 2013. (In Turkish)

* Y. Sabucu and S. Erküçük, Distributed Detection in IEEE 802.15.4a based WSNs, MASFOR, İstanbul, June 2012. (poster presentation)

* Y. Sabucu, T. Çoğalan, A. Küçük and T. Güçlüoğlu, Performance comparisons of coded OFDM systems with antenna selection techniques, Mosharaka International Conference on Communications, Istanbul, 2011.